JACS
JOURNAL OF THE AMERICAN CHEMICAL SOCIETY
pubs.acs.org/JACS



Communication

# Replacing a Cysteine Ligand by Selenocysteine in a [NiFe]-Hydrogenase Unlocks Hydrogen Production Activity and Addresses the Role of Concerted Proton-Coupled Electron Transfer in Electrocatalytic Reversibility

Rhiannon M. Evans,[▽] Natalie Krahn,[▽] Joshua Weiss, Kylie A. Vincent, Dieter Söll, and Fraser A. Armstrong*

Cite This: *J. Am. Chem. Soc.* 2024, 146, 16971−16976

Read Online

ACCESS | Metrics & More | Article Recommendations | Supporting Information

**ABSTRACT:** Hydrogenases catalyze hydrogen/proton interconversion that is normally electrochemically reversible (having minimal overpotential requirement), a special property otherwise almost exclusive to platinum metals. The mechanism of [NiFe]-hydrogenases includes a long-range proton-coupled electron-transfer process involving a specific Ni-coordinated cysteine and the carboxylate of a nearby glutamate. A variant in which this cysteine has been exchanged for selenocysteine displays two distinct changes in electrocatalytic properties, as determined by protein film voltammetry. First, proton reduction, even in the presence of $H_2$ (a strong product inhibitor), is greatly enhanced relative to $H_2$ oxidation: this result parallels a characteristic of natural [NiFeSe]-hydrogenases which are superior $H_2$ production catalysts. Second, an inflection (an *S*-shaped "twist" in the trace) appears around the formal potential, the small overpotentials introduced in each direction (oxidation and reduction) signaling a departure from electrocatalytic reversibility. Concerted proton−electron transfer offers a lower energy pathway compared to stepwise transfers. Given the much lower proton affinity of Se compared to that of S, the inflection provides compelling evidence that concerted proton−electron transfer is important in determining why [NiFe]-hydrogenases are reversible electrocatalysts.

Unlike almost all chemical examples, many redox enzymes behave as efficient *reversible* electrocatalysts when attached to an electrode.[1−5] In electrocatalysis, key parameters are the electron-transfer (ET) steps that determine the electrode potential needed to drive the reaction and non-electron-transfer steps that determine the limiting current magnitude. Sluggish ET introduces an overpotential barrier beyond that required for a reversible process (where the current responds to a minute departure from the formal potential). For electron-transport enzymes, the catalytic cycle includes transfers of electrons and protons, the former by long-range tunneling[6] and the latter by short-range hopping assisted by mobile side chains and water molecules.[7,8] A fundamental requisite for reversible electrocatalysis is the temporal coupling of these transfers to give a concerted proton-coupled electron-transfer (PCET) process.[9−14] Concerted PCET affords a lower activation barrier compared to stepwise reactions, as summarized by Mayer, Hammes-Schiffer, Hammarström, and co-workers.[15−19]

Briefly, transferring an electron and a proton simultaneously to a buried site in a protein diminishes the Born energy penalty and may avoid an electronically unfavorable intermediate. For a bidirectional cyclic process, the advantage is illustrated with a square scheme (Figure 1A) where the options are to go around the square (sequential) or across (concerted).[12] The former imposes an overpotential cost in each direction because electron (or proton) transfers alone produce electrostatically or electronically unstable states, with respective steps being associated with reduction potentials $E$ or $E_H$ and protonation constants $pK_O$ or $pK_R$.

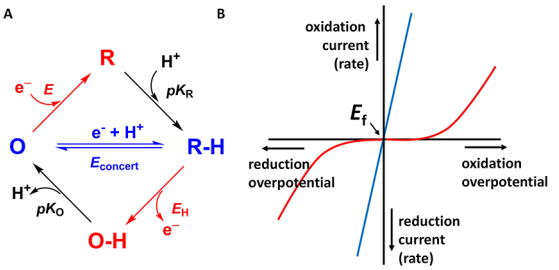


**Figure 1.** (A) Square scheme showing oxidized species O interconverting with reduced species R−H by either a favorable concerted PCET process (blue) or separate steps involving relatively unstable intermediates due to retarded proton transfer (red followed by black). (B) Voltammograms corresponding to the reversible case resulting from concerted PCET (blue) and the irreversible case resulting from electron transfer preceding proton transfer (red): the latter raises the overpotential requirement in each direction. Formal potential indicated as $E_f$.

**Received:** March 11, 2024
**Revised:** May 9, 2024
**Accepted:** May 10, 2024
**Published:** May 15, 2024





https://doi.org/10.1021/jacs.4c03489
*J. Am. Chem. Soc.* 2024, 146, 16971−16976

The difference between concerted and sequential PCET is manifested in the catalytic voltammograms, represented in Figure 1B for a bidirectional system with both oxidized and reduced states being present. A concerted process yields a trace (blue) that cuts sharply through the formal potential, whereas sequential transfers produce an inflection (red) reflecting the additional overpotential needed to drive the reaction in each direction.

Hydrogenases are excellent exemplars of reversible electrocatalysis, their inherent activities being comparable with Pt metals.[20,21] Moreover, they have long been important subjects for protein film electrochemistry (PFE), a suite of techniques providing exquisite, complementary information on redox enzymes.[21−23] For [FeFe]-hydrogenases, much is now established about the mechanism of $H_2$ activation by the active-site H-cluster.[24,25] Experimentally, the specific role of concerted PCET in electrocatalytic reversibility is difficult to isolate among other contributing factors:[1,26] however, for two [FeFe]-hydrogenases, mild disruption of a remote proton-transfer pathway by exchanging a Glu for Asp caused the reversible electrocatalytic trace to become sigmoidal (an inflection appearing in the otherwise continuous potential dependence).[27] Adapting the concept shown in Figure 1, the observations, interpreted as retarded proton mobility, confirmed that *long-range* concerted PCET underpins the reversibility of [FeFe]-hydrogenases.

An interesting case arises for [NiFe]-hydrogenases, where interconversion between $H_2$ and $H^+$ occurs at a site containing a Ni tetrathiolato (four-cysteine) complex linked via two of the cysteine-S atoms to a $Fe^{II}(CN)_2CO$ fragment (Figure 2A).[28]

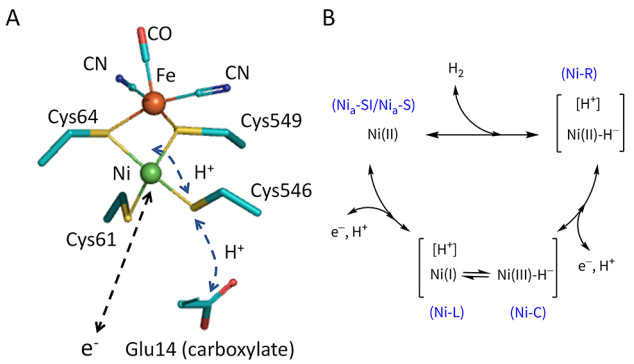


**Figure 2.** (A) Active site of a [NiFe]-hydrogenase, showing the pathway proposed for $H^+$ transfer between its coordination site (as a hydrido ligand) on the Ni atom (Ni−C) via an inner-shell cysteine-S to an outer-shell glutamate and ultimately to solvent. Residues are numbered according to the sequence of *E. coli* Hyd-2. (B) Catalytic cycle showing the oxidation states of intermediates Ni−R, Ni−C, Ni−L, and $Ni_a$−SI ($Ni_{active}$−EPR silent).

During the catalytic cycle summarized in Figure 2B, the Ni atom undergoes changes in the oxidation state (3+, 2+, 1+). There is overwhelming evidence that one or both protons consumed or generated at the active site enter or exit via a pathway comprising nickel-hydrido species, a coordinating (non-bridging) cysteine-S, and the side-chain carboxyl of a glutamate able to approach within H-bonding distance of that specific cysteine S atom.[29−38] A relay pathway is defined for long-range $H^+$ transfer, i.e., solvent ↔ Glu ↔ Cys-S ↔ Ni, as outlined in Figure 2A, based on the structure of Hydrogenase-2 (Hyd-2) from *Escherichia coli*.[39] The electron is transferred to the proximal [4Fe−4S] cluster located approximately 11 Å from the Ni atom.

Our attention focuses on the lower stages of the catalytic cycle involving long-range electron−proton transfer (the upper horizontal process is concerned with H−H bond formation/cleavage and the elusive interaction with the $H_2$ molecule).[40,41] The central (and best characterized) intermediate is a Ni(III)-hydrido species known as Ni−C (isoelectronic with Ni(I)−$H^+$ which corresponds to the R−H species in Figure 1A). The Ni−C state is in tautomeric equilibrium with Ni(I) species known collectively as Ni−L: IR spectroscopic studies have revealed that both Ni−L and Ni−R exist in several forms, differing in the location of the $H^+$ that has migrated locally without leaving the enzyme.[32,33,35,38] The Ni−L species form upon illumination at low temperature, but their detection under normal catalytic conditions has largely been restricted to $O_2$-tolerant [NiFe] hydrogenases, suggesting that the equilibrium otherwise strongly favors Ni−C.[33,38,42,43] During $H_2$ oxidation, Ni−C is converted to a Ni(II) form known as $Ni_a$−SI. Investigations of the Ni−C to $Ni_a$−SI interconversion by transient spectroscopy lend strong support for a concerted process,[31,32] and recent studies of the regulatory hydrogenase from *Cupriavidus necator* by cryo-IR and EPR produced a particularly detailed picture of the proton-transfer steps in that enzyme, elaborating on the pathway shown in Figure 2A.[38]

The crucial cysteine both coordinates Ni and serves as a $H^+$ mediator. An attractive approach for probing the role of a cysteine-S atom is to exchange the cysteine for a selenocysteine (Sec, one-letter code U) by recombinant methods.[44−46] Selenium is only slightly larger than sulfur, and has a similar electronegativity, but its proton affinity is much lower; this property is passed on to Sec, for which the $pK_a$ of the free amino acid is 5.2 compared to 8.3 for Cys.[47−52] In a notable subclass of [NiFe]-hydrogenases, the same cysteine is replaced by selenocysteine: compared to standard [NiFe]-hydrogenases, [NiFeSe]-hydrogenases have higher activity for proton reduction with very little product ($H_2$) inhibition.[53−56] We recently used PFE to investigate the consequences of replacing each of the four Cys coordinating the Ni, by Sec, in the $O_2$-tolerant Hydrogenase-1 (Hyd-1) from *E. coli*.[57] Despite identifying aspects underlying $O_2$ tolerance, we could not address the role of each Sec in catalytic proton transfer because, under neutral pH conditions, Hyd-1 is not a bidirectional catalyst: it catalyzes only irreversible $H_2$ oxidation.[58] We have now made the corresponding Cys-to-Sec exchanges with the counterpart standard hydrogenase of *E. coli*, Hyd-2: unlike Hyd-1, Hyd-2 is a reversible electrocatalyst of the $2H^+/H_2$ reaction, albeit with $H^+$ reduction activity that is strongly inhibited by $H_2$.[39] We could thus determine how each Cys contributes to the *bidirectional* electrocatalytic "signature", interest being focused on Cys-546, implicated in concerted PCET and replaced by Sec in [NiFeSe]-hydrogenases.

To produce Hyd-2 Sec variants, we followed the gene-expression protocol used previously to overproduce native Hyd-2[59] combined with the technology for site-specific Sec insertion.[45] Details are given in the Supporting Information. Hyd-2 was produced from *E. coli* with a chromosomally encoded C-to-U mutant *hyb*C gene and a plasmid encoded, C-terminally hexa-His-tagged *hyb*O gene (pOC)[59] (Figure S1). The Cys codons at positions 61, 64, 546, and 549 in hybC were individually mutated to TAG to create four new *E. coli* strains (Table S1). Transforming these strains with pOC[59] and


https://doi.org/10.1021/jacs.4c03489
J. Am. Chem. Soc. 2024, 146, 16971−16976

pSecUAG-Evol2[45] plasmids yielded final expression strains. Mass spectrometry confirmed maturely processed enzyme with the C-terminal "assembly peptide"[60] missing and Sec insertion at the expected TAG positions (Figure S1). All four variants were active in steady-state $H_2$ oxidation assays, although at lower levels (per mg enzyme) than measured for native Hyd-2 (Table S2).

Despite low yields, definitive observations were made using PFE which requires only minute enzyme quantities and focuses on electrocatalytic signature (reversibility, catalytic bias) rather than absolute activity.[21−23] Catalytic cyclic voltammograms were recorded for native Hyd-2 and each variant, adsorbed at a pyrolytic graphite "edge" (PGE) electrode (Supporting Information). The results are displayed in Figure 3 alongside the corresponding Cys/Sec exchange position. The voltammetry for the C546U variant is markedly different. Under 100% $H_2$, the current due to $H^+$ reduction at −0.2 V vs RHE is larger than that for $H_2$ oxidation at +0.2 V vs RHE: catalytic bias has thus been erased. The comparative result after displacing $H_2$ with Ar shows that $H_2$ is no longer an inhibitor. Close inspection shows that the sharp intersection across the formal $2H^+/H_2$ potential, expected for reversible electrocatalysis and clearly apparent for native Hyd-2 when lower, less inhibitory $H_2$ levels are used (Figure S2),[39,41] is replaced by a subtle inflection. Figure 4 shows that the inflection persists between pH 5 and 8; activity at pH 9 is too low to distinguish the shape. Once most $H_2$ has been replaced by Ar, an inflection is neither expected nor evident, with the greater potential dependence of the $H^+$ reduction rate being the only observable.

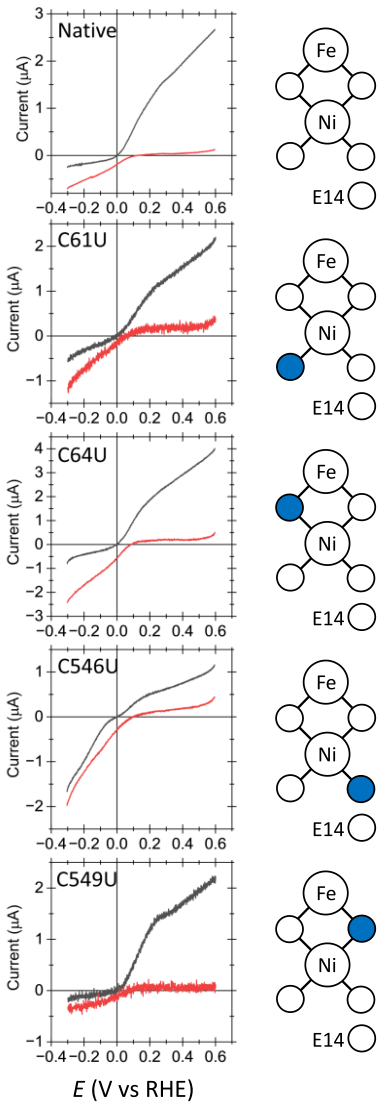


**Figure 3.** Steady-state catalytic voltammograms recorded for Sec variants under 100% $H_2$ (black) and then after replacing the headspace with Ar (red), scan rate 0.5 $mVs^{-1}$. Other conditions: temperature 37 °C; pH = 6.0; electrode rotation rate 1000 rpm. Potential axis has been adjusted to approximate to the reversible hydrogen electrode (RHE) scale.

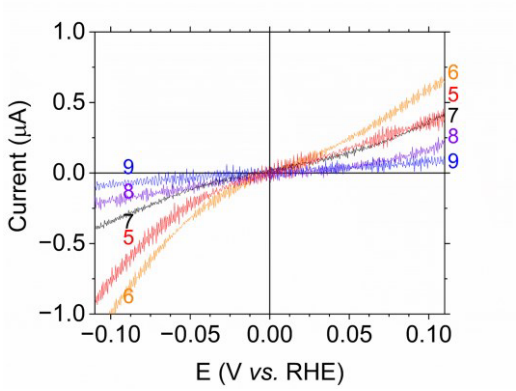


**Figure 4.** Expanded view showing the catalytic voltammograms for $2H^+/H_2$ interconversion by the C546U variant over a range of pH values, at 100% $H_2$, in the reversible region spanning the formal potential. Scan rate 2 mV $s^{-1}$; temperature 37 °C; electrode rotation rate 1000 rpm.

The C546U exchange thus renders Hyd-2 fully bidirectional but with a small but discernible decrease in reversibility. Although substitution of Cys for Sec at this Ni-coordinating site might render electron transfer more sluggish through intractable electronic or structural effects, a more plausible explanation is that electron and proton transfers, occurring in concert (at least for Ni−C to $Ni_a$−SI interconversion),[31,32] have become temporally separated. Aside from inevitable alterations in dynamic local structure, the net impact of which is difficult to predict, the obvious factor is the lower (thermodynamic) proton affinity of Se compared to S, which may override the greater nucleophilicity (kinetic) advantage expected for the former:[48,50,52] compared to thiolate, a selenide base is less able to stabilize $H^+$ in transit. No inflection is observed in PFE studies of natural [NiFeSe]-hydrogenases,[53−55] suggesting other factors ensure that Se imposes no $H^+$ transfer penalty for those enzymes.

Decreased product ($H_2$) inhibition is one reason natural [NiFeSe]-hydrogenases have higher $H_2$ production activities.[53−55] Replacement of S by Se may influence the elusive interaction between Ni and molecular $H_2$ or modify the activity of Ni−R states (one of which may be protonated at C546).[34] For $O_2$-tolerant Hyd-1, the equivalent position was identified to help confer $O_2$ tolerance.[57]

Although at a qualitative stage, the new data establish that long-standing mechanistic hypotheses surrounding [NiFe]- and [NiFeSe]-hydrogenases will be amenable to closer examination once larger quantities of variants can be produced.



https://doi.org/10.1021/jacs.4c03489
J. Am. Chem. Soc. 2024, 146, 16971−16976

The subtle inflection introduced by a specific mutation highlights the influence of concerted proton−electron transfer in minimizing overpotential and achieving reversible electrocatalysis that is so rare in electrochemical research. Even so, we note that it is possible to account for reversible electrocatalysis without explicit consideration of concerted PCET.[26] Finally, with early organisms having a limited thermodynamic range available for electron-transport chains, enzyme structures may have evolved to promote concerted PCET for optimizing efficiency in energy processing. By further refining thermodynamic fitness,[61] *overpotential*, a term otherwise used exclusively by electrochemists, would have been an underlying evolutionary driver.[3]

## ■ ASSOCIATED CONTENT

### Supporting Information

The Supporting Information is available free of charge at https://pubs.acs.org/doi/10.1021/jacs.4c03489.

Plasmid preparation and construction of expression strains, production and characterization of variants, enzyme evaluation, steady-state $H_2$ oxidation activity assays, and electrochemical setup; Table S1: Genotypes of strains created and used in this work; Table S2: Steady-state $H_2$ oxidation activity assays; Figure S1: Hyd-2 active site highlighting the four Cys residues targeted for Sec insertion, SDS-PAGE showing purification of both the large subunit (HybC) and the small subunit (HybO) of Hyd-2 for each of the four Sec variants, and tandem MS data for all four Sec variants; Figure S2: Steady-state catalytic cyclic voltammograms recorded for native Hyd-2 under increasing levels of $H_2$ (PDF)

## ■ AUTHOR INFORMATION


### Corresponding Author

**Fraser A. Armstrong** − *Department of Chemistry, University of Oxford, Oxford OX1 3TA, United Kingdom;* orcid.org/0000-0001-8041-2491; Email: fraser.armstrong@chem.ox.ac.uk

### Authors

**Rhiannon M. Evans** − *Department of Chemistry, University of Oxford, Oxford OX1 3TA, United Kingdom*

**Natalie Krahn** − *Department of Biochemistry and Molecular Biology, University of Georgia, Athens, Georgia 30602, United States;* orcid.org/0000-0003-0696-433X

**Joshua Weiss** − *Department of Biochemistry and Molecular Biology, University of Georgia, Athens, Georgia 30602, United States*

**Kylie A. Vincent** − *Department of Chemistry, University of Oxford, Oxford OX1 3TA, United Kingdom;* orcid.org/0000-0001-6444-9382

**Dieter Söll** − *Department of Molecular Biophysics and Biochemistry, Yale University, New Haven, Connecticut 06511, United States; Department of Chemistry, Yale University, New Haven, Connecticut 06520, United States;* orcid.org/0000-0002-3077-8986

Complete contact information is available at: https://pubs.acs.org/10.1021/jacs.4c03489

### Author Contributions

[▽]R.M.E. and N.K. are equal contributors.


### Notes

The authors declare no competing financial interest.

## ■ ACKNOWLEDGMENTS

This work was supported by the National Institute of General Medical Sciences (R35GM122560, R35GM122560-05S1 to D.S.), the Department of Energy's Office of Basic Energy Sciences (DE-FG02-98ER20311 to D.S.), the European Research Council (Consolidator Grant BiocatSusChem 819580 to K.A.V.), and the UK Biological and Biotechnology Sciences Research Council (BB/I022309-1, BB/L009722/1 to F.A.A.). F.A.A. thanks St John's College, Oxford, for an Emeritus Research Fellowship and Hong Kong University for a Mok Hing-Yiu Distinguished Visiting Professorship. The Orbitrap was purchased with NIH S10RR028859 to Professor I.J. Amster of UGA Chemistry. We thank Chau-Wen Chou from the UGA Proteomics and Mass Spectrometry facility for her expertise and discussion.

## ■ REFERENCES


(1) Armstrong, F. A.; Hirst, J. Reversibility and efficiency in electrocatalytic energy conversion and lessons from enzymes. *Proc. Natl. Acad. Sci. U. S. A.* **2011**, *108*, 14049−14054.

(2) Fourmond, V.; Wiedner, E. S.; Shaw, W. J.; Léger, C. Understanding and Design of Bidirectional and Reversible Catalysts of Multielectron, Multistep Reactions. *J. Am. Chem. Soc.* **2019**, *141*, 11269−11285.

(3) Evans, R. M.; et al. The value of enzymes in solar fuels research - efficient electrocatalysts through evolution. *Chem. Soc. Rev.* **2019**, *48*, 2039−2052.

(4) Fourmond, V.; Plumeré, N.; Léger, C. Reversible catalysis. *Nat. Rev. Chem.* **2021**, *5*, 348−360.

(5) Armstrong, F. A.; Cheng, B.; Herold, R. A.; Megarity, C. F.; Siritanaratkul, B. From Protein Film Electrochemistry to Nano-confined Enzyme Cascades and the Electrochemical Leaf. *Chem. Rev.* **2023**, *123*, 5421−5458.

(6) Winkler, J. R.; Gray, H. B. Long-Range Electron Tunneling. *J. Am. Chem. Soc.* **2014**, *136*, 2930−2939.

(7) Chen, K.; et al. Atomically defined mechanism for proton transfer to a buried redox centre in a protein. *Nature* **2000**, *405*, 814−817.

(8) Shinobu, A.; Agmon, N. Mapping proton wires in proteins: carbonic anhydrase and GFP chromophore biosynthesis. *J. Phys. Chem. A* **2009**, *113*, 7253−7266.

(9) Costentin, C. Electrochemical approach to the mechanistic study of proton-coupled electron transfer. *Chem. Rev.* **2008**, *108*, 2145−2179.

(10) Hammes-Schiffer, S.; Soudackov, A. V. Proton-coupled electron transfer in solution, proteins, and electrochemistry. *J. Phys. Chem. B* **2008**, *112*, 14108−14123.

(11) Yang, J. Y.; et al. Two pathways for electrocatalytic oxidation of hydrogen by a nickel bis(diphosphine) complex with pendant amines in the second coordination sphere. *J. Am. Chem. Soc.* **2013**, *135*, 9700−9712.

(12) Koper, M. T. M. Volcano Activity Relationships for Proton-Coupled Electron Transfer Reactions in Electrocatalysis. *Top. Catal.* **2015**, *58*, 1153−1158.

(13) Warburton, R. E.; Soudackov, A. V.; Hammes-Schiffer, S. Theoretical Modeling of Electrochemical Proton-Coupled Electron Transfer. *Chem. Rev.* **2022**, *122*, 10599−10650.

(14) Nocera, D. G. Proton-Coupled Electron Transfer: The Engine of Energy Conversion and Storage. *J. Am. Chem. Soc.* **2022**, *144*, 1069−1081.

(15) Mayer, J. M.; Rhile, I. J. Thermodynamics and kinetics of proton-coupled electron transfer: stepwise vs. concerted pathways. *Biochimica Et Biophysica Acta-Bioenergetics* **2004**, *1655*, 51−58.

(16) Hammes-Schiffer, S.; Stuchebrukhov, A. A. Theory of coupled electron and proton transfer reactions. *Chem. Rev.* **2010**, *110*, 6939−6960.
(17) Hammes-Schiffer, S. Proton-Coupled Electron Transfer: Moving Together and Charging Forward. *J. Am. Chem. Soc.* **2015**, *137*, 8860−8871.
(18) Tyburski, R.; Liu, T.; Glover, S. D.; Hammarström, L. Proton-Coupled Electron Transfer Guidelines, Fair and Square. *J. Am. Chem. Soc.* **2021**, *143*, 560−576.
(19) Agarwal, R. G.; et al. Free Energies of Proton-Coupled Electron Transfer Reagents and Their Applications. *Chem. Rev.* **2022**, *122*, 1−49.
(20) Jones, A. K.; Sillery, E.; Albracht, S. P.; Armstrong, F. A. Direct comparison of the electrocatalytic oxidation of hydrogen by an enzyme and a platinum catalyst. *Chem. Commun. (Camb)* **2002**, 866−867.
(21) Armstrong, F. A.; et al. Guiding Principles of Hydrogenase Catalysis Instigated and Clarified by Protein Film Electrochemistry. *Acc. Chem. Res.* **2016**, *49*, 884−892.
(22) Fourmond, V.; Léger, C. An introduction to electrochemical methods for the functional analysis of metalloproteins. In *Practical Approaches to Biological Inorganic Chemistry*, 2nd ed.; Elsevier, 2020; pp 325−373; DOI: 10.1016/B978-0-444-64225-7.00009-2.
(23) Butt, J. N.; Jeuken, L. J. C.; Zhang, H. J.; Burton, J. A. J.; Sutton-Cook, A. L. Protein film electrochemistry. *Nat. Rev. Method Prime* **2023**, *3*, 7710.
(24) Birrell, J. A.; Rodríguez-Maciá, P.; Reijerse, E. J.; Martini, M. A.; Lubitz, W. The catalytic cycle of [FeFe] hydrogenase: A tale of two sites. *Coordin Chem. Rev.* **2021**, *449*, 214191.
(25) Tai, H.; Hirota, S.; Stripp, S. T. Proton Transfer Mechanisms in Bimetallic Hydrogenases. *Acc. Chem. Res.* **2021**, *54*, 232−241.
(26) Fasano, A.; et al. Kinetic Modeling of the Reversible or Irreversible Electrochemical Responses of FeFe-Hydrogenases. *J. Am. Chem. Soc.* **2024**, *146*, 1455−1466.
(27) Lampret, O.; et al. The roles of long-range proton-coupled electron transfer in the directionality and efficiency of [FeFe]-hydrogenases. *Proc. Natl. Acad. Sci. U. S. A.* **2020**, *117*, 20520−20529.
(28) Pandelia, M. E.; Ogata, H.; Lubitz, W. Intermediates in the catalytic cycle of [NiFe] hydrogenase: functional spectroscopy of the active site. *ChemPhysChem* **2010**, *11*, 1127−1140.
(29) Brown, L. S.; et al. Glutamic acid 204 is the terminal proton release group at the extracellular surface of bacteriorhodopsin. *J. Biol. Chem.* **1995**, *270*, 27122−27126.
(30) Dementin, S.; et al. A glutamate is the essential proton transfer gate during the catalytic cycle of the [NiFe] hydrogenase. *J. Biol. Chem.* **2004**, *279*, 10508−10513.
(31) Greene, B. L.; Wu, C. H.; McTernan, P. M.; Adams, M. W.; Dyer, R. B. Proton-coupled electron transfer dynamics in the catalytic mechanism of a [NiFe]-hydrogenase. *J. Am. Chem. Soc.* **2015**, *137*, 4558−4566.
(32) Greene, B. L.; Vansuch, G. E.; Wu, C. H.; Adams, M. W.; Dyer, R. B. Glutamate Gated Proton-Coupled Electron Transfer Activity of a [NiFe]-Hydrogenase. *J. Am. Chem. Soc.* **2016**, *138*, 13013−13021.
(33) Ash, P. A.; Hidalgo, R.; Vincent, K. A. Proton Transfer in the Catalytic Cycle of [NiFe] Hydrogenases: Insight from Vibrational Spectroscopy. *ACS Catal.* **2017**, *7*, 2471−2485.
(34) Dong, G.; Ryde, U. Protonation states of intermediates in the reaction mechanism of [NiFe] hydrogenase studied by computational methods. *J. Biol. Inorg. Chem.* **2016**, *21*, 383−394.
(35) Greene, B. L.; Wu, C. H.; Vansuch, G. E.; Adams, M. W.; Dyer, R. B. Proton Inventory and Dynamics in the Nia-S to Nia-C Transition of a [NiFe] Hydrogenase. *Biochemistry* **2016**, *55*, 1813−1825.
(36) Evans, R. M.; et al. Mechanistic Exploitation of a Self-Repairing, Blocked Proton Transfer Pathway in an O(2)-Tolerant [NiFe]-Hydrogenase. *J. Am. Chem. Soc.* **2018**, *140*, 10208−10220.
(37) Tai, H.; Nishikawa, K.; Higuchi, Y.; Mao, Z. W.; Hirota, S. Cysteine SH and Glutamate COOH Contributions to [NiFe] Hydrogenase Proton Transfer Revealed by Highly Sensitive FTIR Spectroscopy. *Angew. Chem., Int. Ed. Engl.* **2019**, *58*, 13285−13290.
(38) Waffo, A. F. T.; Lorent, C.; Katz, S.; Schoknecht, J.; Lenz, O.; Zebger, I.; Caserta, G.; et al. Structural Determinants of the Catalytic Ni(a)-L Intermediate of [NiFe]-Hydrogenase. *J. Am. Chem. Soc.* **2023**, *145*, 13674−13685.
(39) Lukey, M. J.; et al. How Escherichia coli is equipped to oxidize hydrogen under different redox conditions. *J. Biol. Chem.* **2010**, *285*, 3928−3938.
(40) Evans, R. M.; et al. Mechanism of hydrogen activation by [NiFe] hydrogenases. *Nat. Chem. Biol.* **2016**, *12*, 46−50.
(41) Evans, R. M.; et al. Comprehensive structural, infrared spectroscopic and kinetic investigations of the roles of the active-site arginine in bidirectional hydrogen activation by the [NiFe]-hydrogenase 'Hyd-2' from Escherichia coli. *Chem. Sci.* **2023**, *14*, 8531−8551.
(42) Murphy, B. J.; et al. Discovery of Dark pH-Dependent H(+) Migration in a [NiFe]-Hydrogenase and Its Mechanistic Relevance: Mobilizing the Hydrido Ligand of the Ni-C Intermediate. *J. Am. Chem. Soc.* **2015**, *137*, 8484−8489.
(43) Hidalgo, R.; Ash, P. A.; Healy, A. J.; Vincent, K. A. Infrared Spectroscopy During Electrocatalytic Turnover Reveals the Ni-L Active Site State During H2 Oxidation by a NiFe Hydrogenase. *Angew. Chem., Int. Ed. Engl.* **2015**, *54*, 7110−7113.
(44) Ambrogelly, A.; Palioura, S.; Söll, D. Natural expansion of the genetic code. *Nat. Chem. Biol.* **2007**, *3*, 29−35.
(45) Mukai, T.; Sevostyanova, A.; Suzuki, T.; Fu, X.; Söll, D. A Facile Method for Producing Selenocysteine-Containing Proteins. *Angew. Chem., Int. Ed.* **2018**, *57*, 7215−7219.
(46) Chung, C. Z.; Miller, C.; Söll, D.; Krahn, N. Introducing Selenocysteine into Recombinant Proteins in Escherichia coli. *Curr. Protoc* **2021**, *1*, No. e54.
(47) Noguera, M.; Rodríguez-Santiago, L.; Sodupe, M.; Bertran, J. Protonation of glycine, serine and cysteine.: Conformations, proton affinities and intrinsic basicities. *J. Mol. Struc-Theochem* **2001**, *537*, 307−318.
(48) Wessjohann, L. A.; Schneider, A.; Abbas, M.; Brandt, W. Selenium in chemistry and biochemistry in comparison to sulfur. *Biol. Chem.* **2007**, *388*, 997−1006.
(49) Steinmann, D.; Nauser, T.; Koppenol, W. H. Selenium and sulfur in exchange reactions: a comparative study. *J. Org. Chem.* **2010**, *75*, 6696−6699.
(50) Maroney, M. J.; Hondal, R. J. Selenium versus sulfur: Reversibility of chemical reactions and resistance to permanent oxidation in proteins and nucleic acids. *Free Radic Biol. Med.* **2018**, *127*, 228−237.
(51) Maia, L. B.; Maiti, B. K.; Moura, I.; Moura, J. J. G. Selenium-More than Just a Fortuitous Sulfur Substitute in Redox Biology. *Molecules* **2024**, *29*, 120.
(52) Reich, H. J.; Hondal, R. J. Why Nature Chose Selenium. *ACS Chem. Biol.* **2016**, *11*, 821−841.
(53) Parkin, A.; Goldet, G.; Cavazza, C.; Fontecilla-Camps, J. C.; Armstrong, F. A. The difference a Se makes?: Oxygen-tolerant hydrogen production by the [NiFeSe]-hydrogenase from. *J. Am. Chem. Soc.* **2008**, *130*, 13410−13416.
(54) Riethausen, J.; Rudiger, O.; Gartner, W.; Lubitz, W.; Shafaat, H. S. Spectroscopic and electrochemical characterization of the [NiFeSe] hydrogenase from Desulfovibrio vulgaris Miyazaki F: reversible redox behavior and interactions between electron transfer centers. *Chembiochem* **2013**, *14*, 1714−1719.
(55) Wombwell, C.; Caputo, C. A.; Reisner, E. [NiFeSe]-hydrogenase chemistry. *Acc. Chem. Res.* **2015**, *48*, 2858−2865.
(56) Marques, M. C.; et al. The direct role of selenocysteine in [NiFeSe] hydrogenase maturation and catalysis. *Nat. Chem. Biol.* **2017**, *13*, 544−550.
(57) Evans, R. M. Selective cysteine-to-selenocysteine changes in a [NiFe]-hydrogenase confirm a special position for catalysis and oxygen tolerance. *Proc. Natl. Acad. Sci. U. S. A.* **2021**, *118*, e2100921118.

(58) Murphy, B. J.; Sargent, F.; Armstrong, F. A. Transforming an oxygen-tolerant [NiFe] uptake hydrogenase into a proficient, reversible hydrogen producer. *Energ Environ. Sci.* **2014**, *7*, 1426−1433.
(59) Beaton, S. E.; et al. The structure of hydrogenase-2 from Escherichia coli: implications for H(2)-driven proton pumping. *Biochem. J.* **2018**, *475*, 1353−1370.
(60) Dubini, A.; Sargent, F. Assembly of Tat-dependent [NiFe] hydrogenases: identification of precursor-binding accessory proteins. *FEBS Lett.* **2003**, *549*, 141−146.
(61) McGuinness, K. N.; et al. The energetics and evolution of oxidoreductases in deep time. *Proteins* **2024**, *92*, 52−59.



https://doi.org/10.1021/jacs.4c03489
*J. Am. Chem. Soc.* 2024, 146, 16971−16976